Characterization of Biodegradable Polymers by Inverse Gas Chromatography. III. Blends of Amylopectin and Poly(L-lactide)

Bihuan Zhong, Zeki Y. Al-Saigh

Department of Chemistry, State University of New York College at Buffalo, Buffalo, NY 14222

Received 9 November 2010; accepted 15 March 2011
DOI 10.1002/app.34516
Published online 31 August 2011 in Wiley Online Library (wileyonlinelibrary.com).

ABSTRACT: The morphology changes and surface thermodynamics of blends of amylopectin (AP)–poly(L-lactide) (PLA) were investigated over a wide range of temperatures and compositions using the inverse gas chromatography method. Twenty-five solutes were selected such as alkanes, acetates, oxy, halogenated, and six-member ring families. They provided a variety of specific interactions with the blends' surface. The morphology showed two regions, some others showed a de-polymerization above 130°C. These zones enabled the estimation of T_g and T_m of AP, PLA, and the blends. Blending AP with PLA caused a decrease in AP's T_g value due to the reduction of the degree of crystallinity of the blend. Exothermic values of χ_{23} were obtained indicating the compatibility of AP and PLA at all temperatures and weight fractions of AP–PLA. The miscibility was favored at 75%AP, only 25%AP–75%PLA composition influenced the degree of crystallinity. The dispersive component of the surface energy of the blends ranged from 16.09 mJ/m^2 for the pure AP as high as 58.36 mJ/m^2 at 110°C when AP was mixed with PLA in a 50–50% ratio. The surface energy was at its highest value when the composition was 75% of AP, in good agreement with χ_{23} values. J Appl Polym Sci 123: 2616–2627, 2012

Key words: amylopectin; poly(L-lactide); inverse gas chromatography; degree of crystallinity; surface energy; interaction coefficients; differential scanning calorimetry; X-ray diffraction; polymer–polymer interaction; entropy of mixing

INTRODUCTION

In our recent paper in this *Journal*, we reported[1] the possibility of improving starch's physicochemical properties by blending it with a compatible biodegradable polymer. Starch and its blends have attracted much attention as environmentally biodegradable polymers.[2–4] The blending process resulted in an exothermic heat of mixing, lower starch crystallinity and a higher dispersive component of the surface energy as determined by the inverse gas chromatography (IGC) method. However, starch suffers from disadvantages as compared with the conventional polymers and blends such as brittleness and a narrow processability window.[2] Amylopectin (AP) as a potato starch contains 25% amylase; both AP and amylase create a system that does not enhance strong interactions to evolve good mechanical properties.[5] Because the world is experiencing an excessive consumption of nonrenewable fossil oil resources, our interest in starch-biodegradable polymer blends as potential renewable resources. Several methods were used for the characterization of these materials such as: differential scanning calorimetry (DSC), Fourier transform infrared spectroscopy, scanning electron microscopy solvent extraction, X-ray diffraction, optical rotation, nuclear magnetic resonance, polarizing optical microscopy,[6–9] and IGC.[10,11]

IGC stands out among other techniques because of its convenience for the characterization of surface and bulk properties of solids and blends.[12] In addition, it is a cost-effective method, reliable, and fast in obtaining accurate data. Being the reverse of a conventional gas chromatographic (GC) experiment, the interest is the analysis of the stationary phase rather than the mobile phase. In IGC experiments, the polymeric system under study is usually coated on a solid support and uniformly packed in a chromatographic column. IGC has proved to be a powerful tool for the characterization of solid surfaces like, fibers or powders; particularly those that cannot be easily studied by other methods.[12–25] IGC was also used to characterize the surface properties of pharmaceutical powders[26] and cellulose fibers.[27,28] A review on the applicability of the IGC technique for the characterization of physicochemical properties of starch–polymer blends materials was recently made by Al-Saigh.[29]

Correspondence to: Z. Y. Al-Saigh (ALSAIGZY@Buffalostate.edu).

Our interest stems from the fact that both AP and poly(L-lactide) (PLA) are biodegradable and both are from renewable sources. PLA has been an industrial commodity with important applications, particularly in packaging and fiber technology. PLA is one of the most commonly used biodegradable polymers. It is produced from L-lactic acid, which is derived from the fermentation of corn or sugar beets, or it can be made by ring opening polymerization from L-lactide. It is synthesized from optically active L-lactic acid by a stereo-controlled polymerization process. PLAs biodegradation ability presents the major advantage to enter into the natural cycle, implying its return to the biomass. PLA is a relatively stiff, crystalline and brittle polymer with low deformation at break.

In this work, IGC will predict whether blends of AP and PLA are miscible and whether the physicochemical properties of the blend have improved as compared with those of pure AP properties. Such improvement may shed the light on the future development of plastics made from starch–polymer blends with stronger mechanical properties.

Thermodynamics of IGC

A complete analysis of the thermodynamics of IGC was recently reviewed.[12,29] The key term in IGC experiments is the specific retention volume V_g^o, which enables the determination of thermodynamic parameters of a system under study, degree of crystallinity, and the dispersive component of the surface energy. By measuring several main experimental chromatographic quantities such as the flow rate, column temperature, retention time of solutes, mass of the polymer, and the pressures of the carrier gas at the inlet and the outlet of the column, V_g^o can be calculated as follows:

$$V_g^o = \frac{273.15 \Delta t F J}{w T_c} \tag{1}$$

J is the correction for the compressibility of the carrier gas across the chromatographic column defined by the following relation:

$$J = \frac{3}{2}\left[\frac{\left(\frac{P_i}{P_o}\right)^2 - 1}{\left(\frac{P_i}{P_o}\right)^3 - 1}\right]. \tag{2}$$

Here, $\Delta t = t_p - t_m$ is the difference between the retention time of the solute, t_p, and of the marker, t_m. Air is usually used as a marker to account for the dead volume in the chromatographic column when the thermal conductivity (TC) detector is used. The retention time of the marker has to be subtracted from the solute retention time to reflect the absolute value of the solute retention time as Δt. F is the flow rate of the carrier gas measured at the column temperature T_c, and w is the mass of the stationary phase. J factor is calculated using P_i and P_o, the inlet and outlet pressures, respectively. P_i and P_o are measured using electronic transducers, which are interfaced at the inlet and outlet of the column. These transducers are usually calibrated using a mercury manometer. Because Δt is a function of F, it has to be extrapolated to F to reflect the true value of Δt. Then, the product of the Δt and the flow rate F may also yield a valuable quantity as a net retention volume, V_N, as follows:

$$V_N = \Delta t F \tag{3}$$

V_N in Eq. (3) accounts for the retention time of solute in terms of volume in milliliters and it is dependent on the mass of the polymer in the column. To be more specific, V_N can be taken a step further by dividing it by the mass of the polymer and corrected to 0°C to become a specific retention volume of the solute, V_g^o as in Eq. (1).

$$V_g^o = V_N\left(\frac{273.15}{wTc}\right) \tag{4}$$

V_g^o also enable the calculations of the partition coefficient, K_p, which will lead to the calculation of the molar free energy of adsorption (ΔG_s) of the solutes into the polymer layer, using the following relationship:

$$K_p = \frac{V_g^o \rho T}{273.12} \tag{5}$$

where ρ is the density of the polymer in the chromatographic column. Then, the relationship between K_p and the ΔG_s is well known:

$$\Delta G_s = -RT \ln K_p. \tag{6}$$

Accordingly, the molar heat of sorption (ΔH_s^1) of solutes into the polymer layer can also be derived from IGC data as follows.[30] For a pure solvent, the liquid–vapor equilibrium is described by the Clapeyron equation:

$$\frac{dP}{dT} = \frac{\Delta H_{\text{ad}}^1}{T\left(\bar{V}_g - \bar{V}_l\right)}. \tag{7}$$

Here, $\overline{V}_g$ and $\overline{V}_l$ are partial molar volumes of the solute gas and liquid states and ΔH_{ad}^1 is the partial molar heat of adsorption of the solute onto the polymeric surface. An analogous relation can be derived for sorption of solutes into the polymer layer (ΔH_s^1):

$$\frac{\partial P_1}{\partial T} = \frac{\Delta H_s^1}{T\left(\bar{V}_g - \bar{V}_l\right)}. \tag{8}$$

Considering that $\overline{V}_l$ is negligible as compared with $\overline{V}_g$ and substituting the pressure of the vapor from the ideal gas equation for $P_1 = \frac{RT}{V_g}$ (this always allowed in IGC at infinite solution), Eq. (9) can be derived as:

$$d \ln V_g^o d\left(\frac{1}{T}\right) = -\frac{\Delta H_s^1}{R}. \quad (9)$$

A plot of ln V_g^o versus the inverse of temperature will determine ΔH_s^1. If the polymer surface is amorphous at the experiment's temperature, the equilibrium between the vapor and the polymer will be established, then the slope of the linear relationship.

$$\Delta H_s^1 = -\left[\frac{R\partial \ln V_g^o}{\partial(1/T)}\right]. \quad (10)$$

To calculate the interaction parameter of each solute used with the pure polymer, V_g^o from Eq. (1) can also be utilized to calculate the interaction parameter as, χ_{12}, of the starch–solute and poly(lactic acid)–solute and blend–solute systems, as follows:

$$\chi_{12} = \ln\frac{273.15R\nu_2}{V_g^o V_1 P_1^o} - 1 + \frac{V_1}{M_2\nu_2} - \frac{B_{11} - V_1}{RT}P_1^o \quad (11)$$

χ_{12} parameter can reveal the strength of the specific interactions between the solutes and the pure polymers and with the polymer pair. 1 denotes the solute and 2 denotes the polymer under examination; υ_2 is the specific volume of the polymer at the column temperature T_c; M_1 is the molecular weight of the solute; P_1^o is the saturated vapor pressure of the solute; V_1 is the molar volume of the solute; R is the gas constant; and B_{11} is the second virial coefficient of the solute in the gaseous state. Equation (11) is used routinely for the calculation of χ_{12} from IGC experiments.

As we reported in series I,[1] when two polymers are blended, we will refer to the blend as the polymer pair. In this case, the key term in determining the miscibility of a polymer pair is the free energy of mixing, ΔG_m as:

$$\Delta G_m = \Delta H_m - T\Delta S_m. \quad (12)$$

We also reported in the same article the role of the combinatorial entropy of mixing, ΔS_m and the molar heat of mixing, ΔH_m, in the mixing process of the two polymers according to Flory.[31] Accordingly, in our case, only the value of ΔH_m describes the miscibility of the polymer pairs. The volume fraction term φ_i of an individual polymer i was first introduced by Flory and Huggins theory,[31] as described in the following equation:

$$\Delta G_{\text{mix}} = RT\{n_1 \ln \varphi_1 + n_2 \ln \varphi_2 + n_1\varphi_2\chi_{12}\} \quad (13)$$

where n_i is the number of moles of the ith component, RT is the product of the universal gas constant and the absolute temperature, and χ_{12} is the enthalpic contact parameter derived in Eq. (11), which is inversely proportional to absolute temperature. The first two logarithmic terms in Eq. (13) represent the (combinatorial) entropy of mixing. Although the sign of the combinatorial entropy always favors mixing, it is clear that its magnitude is greatly diminished as molar volumes become very large.

In our earlier publications,[25] we derived an equation for the calculation of the polymer–polymer interaction coefficient, χ_{23}, utilizing V_g^o calculated from Eq. (1). When a polymer pair is used as a stationary (liquid) phase in a chromatographic column, ΔG_{mix}, acts as a measure of the interactions between the two polymers and expressed in terms of the free energy of mixing Eq. (12). The subscripts 2 and 3 will be used to represent polymers 1 and 2, respectively. Subscript 1 refers to the test solute. ΔG_{mix} has the same form as Eq. (13), except the subscripts change to 2 and 3. The first two (entropic) terms in this equation are negligible for polymer blends. Thus, for a polymer blend to be miscible (ΔG_{mix} being negative), χ_{23} must be negative. When considering IGC of polymer blends, the free energy of mixing must be written for a three-component system. It is usually expressed in Eq. (14):

$$\Delta G_{\text{mix}} = RT[n_1 \ln \phi_1 + n_2 \ln \phi_2 + n_3 \ln \phi_3 + n_1\phi_2\chi_{12} + n_1\phi_3\chi_{13} + n_2\phi_3\chi_{23}], \quad (14)$$

when a polymer blend is used as a stationary phase in a chromatographic column, then the interaction between the two polymers is expressed in terms of χ_{23}, Eq. (14), as an indicator of the miscibility of a polymer blend. If χ_{23} is negative, then the polymer pair is miscible. Recognizing that for a polymer blend containing polymer 1 and polymer 2, υ_2 in Eq. (11) should be replaced by ($w_2\,\upsilon_2 + w_3\,\upsilon_3$), where w_2 and w_3 are the weight fractions and υ_2 and υ_3 are the specific volumes of the two polymers in the blend, the χ_{23} can be derived from:

$$\chi_{23} = \frac{\ln\frac{V^0_{g,\text{blend}}}{W_2\nu_2 + W_3\nu_3} - \phi_2 \ln\frac{V^0_{g,2}}{\nu_2} - \phi_2 \ln\frac{V^0_{g,3}}{\nu_3}}{\phi_2\phi_3}. \quad (15)$$

Equation (15) was first derived by us,[25] where ϕ_2 and ϕ_3 are the volume fractions of the two polymers in the blend. To obtain χ_{23} for a polymer blend, utilizing IGC, χ_{12} and χ_{13} have to be known for pure polymer 1 and 2. Three columns are usually prepared; two from the pure homopolymers (2 and 3) and the third from a blend of the polymer pair (blend).

Furthermore, three more columns containing different compositions of the blend can also be prepared if the effect of the weight fraction of the blend on the miscibility needs to be explored. These columns were studied under identical conditions of column temperature, carrier gas flow rate, inlet pressure of the carrier gas, and the same solutes. Thus, at high molecular weights, only a negative χ_{23} parameter satisfies the condition for miscibility of a polymer pair.

A complete theoretical treatment for the calculation of the dispersive component of the surface energy of polymers using alkanes was published elsewhere.[32,33] According to Fowkes,[33] two components contribute to the surface energy depending on the polarity of the mobile phase; polar (γ_p) and nonpolar or dispersive (γ_d). When the mobile gaseous phase comes in contact with the polymeric surface, an interfacial energy will be created according to the individual surface energy and the polarity of the mobile phase. Then, the adsorption of the solute vapor onto the polymer surface will be affected by the magnitude of the surface free energy.

Again, V_g^o values from Eq. (1) can be utilized in the calculation of the equilibrium constant K between the adsorbed solute and the polymer surface and the free energy of adsorption of vapor on the polymer surface, ΔG_1^s, as follows:

$$\Delta G_1^s = -RT \ln V_g^o + C. \tag{16}$$

Equation (17) relates the energy of adsorption to the surface energy as follows:

$$RT \ln V_g^o + C = 2\mathrm{Na}\sqrt{\gamma_s^d \gamma_i^d} \tag{17}$$

where γ_s^d and γ_i^d are the dispersive components of the solid surface and the interactive solutes phase, respectively. Equation (17) can be rewritten to yield the dispersive surface energy as follows:

$$\gamma_s^d = \left[\frac{1}{4\gamma_{\mathrm{CH_2}}}\right]\left[\frac{\left(\Delta G_a^{\mathrm{CH2}}\right)^2}{\left(Na_{\mathrm{CH2}}\right)^2}\right] \tag{18}$$

where $\gamma_{\mathrm{CH_2}}$ is the surface energy of a hydrocarbon consisting only of *n*-alkanes, a_{CH2} is the area of one —CH2 group. Equation (18) will be routinely used to obtain the dispersive surface energy of polymers.

EXPERIMENTAL

Materials

AP was purchased from Sigma-Aldrich, USA, with a molar mass of 6.60×10^6 gram/mol as a potato starch. It contains 25% amylase. PLA was purchased from Sigma-Aldrich, USA, with M_w of 100 to 150 $\times$ 10^3 gram/mol as reported by Sigma-Aldrich using GPC. It has a glass transition temperature around 48.5°C and inherent viscosity of 0.90–1.20 dL/g. A series of families of solvents with a different chemical nature called "solutes" were selected to interact with the blend of AP–PLA. A total of 25 solutes are used (Table I). They represent five different families: alkanes, acetates, oxy, halogenated, and six-member ring. Each solute is assigned a code and programmed to allow the calculations of molar volume, saturated vapor pressure, gas and liquid densities, and B_{11} parameter. Each group was selected from solutes with an increasing number of carbons in the solutes backbone. Thus, alkanes reveal the effect of its dispersive forces on the solubility with pure PA, PLA, and AP–PLA blend and allow the calculations of the dispersive surface energy of these polymers. Acetates will reveal the effect of dipole–dipole and H-bonding, Halogenated and oxy families will reveal the effect of H-bonding. Aromatic and cyclic families will reveal the effect of Van der Waal's interactions on the solubility of these polymers. Their different interactions with the stationary phase will reveal the effect of the different chemical nature of the injected solutes on the thermodynamic parameters, χ_{12}, χ_{13}, and χ_{23} of these polymers. All 25 solutes as chromatographic grade were purchased from Sigma-Aldrich, USA, as HPLC grade. Their purity was checked by gas chromatography prior to use. An inert chromatographic support, Chromosorb W (AW-DMCS treated, 60/80 mesh) was obtained from Restek.

Instrumentation and procedure

A complete description of the instrumental set-up was outlined in our first series.[10] Chromatographic measurements were made using an IGC Station, consisting of a modified Varian model 3800P. The chromatograph was equipped with a TC detector and was modified to minimize the instrumental artifacts in the measurement of the chromatographic quantities used in Eq. (1), such as the carrier gas flow rate,[34] the inlet and outlet pressure, and the column temperature.[25] Varian 3800P is fully automated and equipped with flow rate fluctuation correction controlled by STAR software. Data handling and analysis of both chromatographs were made possible by special home customized programs; created to enable the variety of thermodynamic calculations used by the IGC Method. To eliminate the contribution of the "inert" solid support to the retention volume, measurements of all 25 solutes were made using a blank chromatographic column packed with only the solid support (0% loading). The retention time of each solute was subtracted from the net retention volume illustrated in Eq. (1). The retention volumes

TABLE I
Families of 25 Solutes with Different Chemical Nature

Families' name	Solutes' name	Code used in this work
Alkanes	*n*-Hexane	NC6
	n-Heptane	NC7
	n-Octane	NC8
	n-Nonane	NC9
	n-Decane	C10
	n-Undecane	C11
	n-Dodecane	C12
Acetates	Methyl acetate	MAC
	Ethyl acetate	EAC
	Propyl acetate	PAC
	n-Butyl acetate	NBA
Oxy group	Tetrahydrofuran	THF
	Dioxane	DOX
	Acetone	ACT
	Methyl ethyl ketone	MEK
Halogenated group	Methylene chloride	CL2
	Trichloro ethylene	TCE
	Chloroform	CL3
	Chlorobenzene	CLB
	Pentyl chloride	PCL
	Butyl chloride	BCL
	1,2-dichloroethane	D12
Six-membered ring group	Cyclohexene	CHX
	Benzene	CC6
	Toluene	TOL

of solutes on a zero loading column (support only) were saved in a separate file and interpolated over a wide range of temperatures, then subtracted from those measured on loaded columns. This automated system was fast and ideal for routine IGC measurements.

Vanishingly small amounts (0.20 μL) of a series of the selected solutes were injected into the chromatographic column. This small volume has been tested to yield an absolute value of solutes' retention volumes. Chromatographic columns were made in the laboratory from 5-ft-long, copper tubing, 1/4 in. in o.d. All copper columns were washed with methanol and annealed for several hours before use. Five chromatographic columns were prepared from five solutions containing different weight fractions of the blend. Each solution was prepared by dissolving a certain amount of AP and PLA in the appropriate solvent and deposited onto 7.921 g Chromosorb W using a soaking method developed by us earlier.[25] The resulting load of the AP–PLA on the column was maintained at around 6.30% to ensure column porosity. Full descriptions of these columns are illustrated in Table II. All columns were studied under identical conditions of temperature, flow rate, inlet, and outlet pressure of the carrier gas. Experiments were performed with 10°C increments starting at 80°C. Columns' temperatures operated continuously and increased upward to eliminate the possibility of recrystallization if they were cooled until this study is complete.

RESULTS AND DISCUSSION

IGC retention diagrams

We reported recently the morphology changes and the thermal analysis of pure AP with a molecular weight of 6×10^6 gram/mol by using DSC and TGA methods.[10] IGC complimented the DSC and TGA findings by identifying the glass transition and melting temperatures.[1] Our findings show that IGC is capable (as the DSC method) of analyzing the morphology of a polymeric system as a function of temperature. From IGC experiments, retention diagrams (thermal isotherms) of the polymeric system can be generated using the V_g^o values [Eq. (1)]. Using Eq. (10), $\ln V_g^o$ of each solute series was plotted versus $1/T$ to generate the retention diagram of that series. If the polymer is semicrystalline, the isotherm is expected to contain several thermal changes due to the change in the morphology of the crystalline polymer as temperature increases. In our case, both AP and PLA are semicrystalline, thus, retention diagrams of pure AP, pure PLA, and the blend of the polymer pair are expected to show at least two zones: crystalline and amorphous zones. The detection of these zones will enable the estimation of the glass transition and the melting temperatures of AP, PLA, and the blend. Indeed, most solutes retention diagrams showed the two regions, some others showed a third region above 130°C which was identified as the de-polymerization zone when the polymer starts to decompose. Figures 1–3 are

TABLE II
Chromatographic Columns Description

Type	Wt. of AP	Wt. of PCL	Volume fraction AP	Volume fraction PLA	Solvent	Wt. of support	% Loading
100% AP	0.4940 g	0.00 g	1.00	0.00	Methanol	7.921 g	6.24%
100% PLA	0.00 g	0.4974 g	0.00	1.00	Chloroform	7.921 g	6.28%
25–75% AP-PCL	0.1260 g	0.3741 g	0.2260	0.7742	Chloroform + Methanol	7.921 g	6.31%
50–50% AP-PCL	0.2528 g	0.2532 g	0.4635	0.5365	Chloroform + Methanol	7.921 g	6.39%
75–25% AP-PCL	0.3757 g	0.1257 g	0.27212	0.2788	Chloroform + Methanol	7.921 g	6.33%

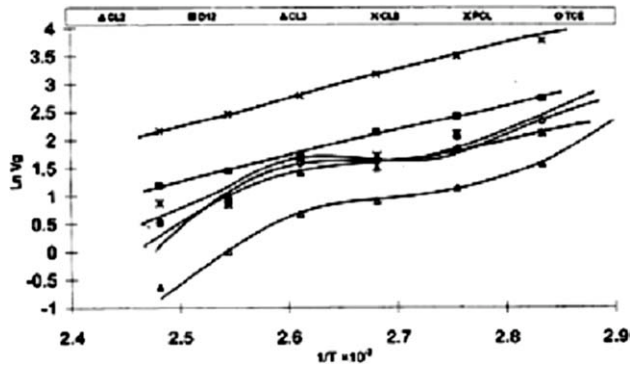

Figure 1 Retention diagram of pure PLA–halogenated solutes (80–130°C).

representative of the retention diagrams for pure PLA using acetates, alkanes and halogenated solutes. Figure 4 is the retention diagram of pure AP using oxy solutes. Figures 5–7 are representative of the retention diagrams of three compositions (25–75%, 50–50%, and 75–25%) of AP–PLA blends using alkanes and acetates. Retention diagrams show that PLA and the blend decomposed above 130°C (Fig. 3); hence, experiments were not performed above 130°C to avoid clogging the column. Retention diagrams of pure AP–alkanes and acetates system were published by us elsewhere;[10] however, the retention diagrams of AP–oxy group, halogenated, and cyclic solutes were generated in this work. Figure 4 shows clear morphology changes of AP as temperatures increased to 200°C using the oxy group. Because AP decomposes at a temperature higher than 170°C, IGC experiments were extended up to 200°C. Pronounced thermal transitions were detected that enabled the determination of T_m and T_g of AP (Table III). By examining the thermal changes of all polymers involved, an estimation of T_m and T_g can be made. In the past,[9] IGC has determined that pure AP has a glass transition temperature (T_g) of 105°C and a melting temperature (T_m) of 166°C, in agreement with the DSC method. Notice that the blends

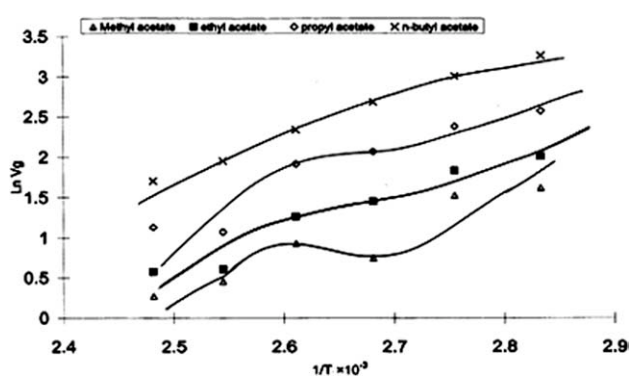

Figure 2 Retention diagram of pure PLA–acetates solutes (80–130°C).

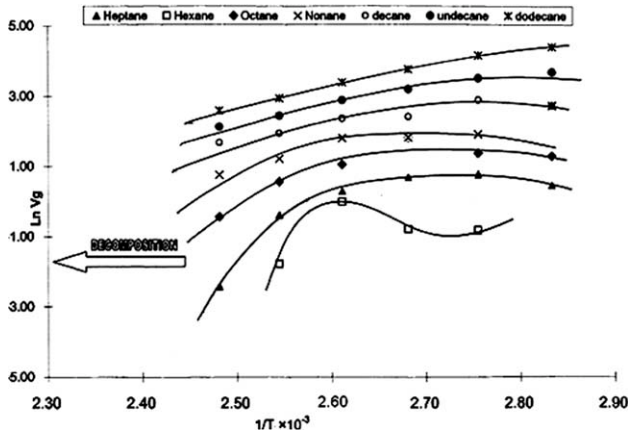

Figure 3 Retention diagram of pure PLA–alkanes solutes (80–130°C).

diagrams show thermal transition as a function of composition of the blend and they are different from that for pure AP and PLA. It is interesting to note that polar solute families (acetates and halogenated) showed more pronounced thermal changes than the nonpolar solutes such as alkanes due to the strong interaction with the surface. This observation measured the strength of the interaction forces developed between the mobile phase and the polymers used. This observation is further acknowledged in the following section.

From all retention diagrams of solute series, the melting temperatures of AP, PLA, and three compositions of the blends were measured (Table III). T_m values agreed well among the solutes families for PLA and the blends, except for AP in which the alkanes and acetates yielded closer T_m values to the published one by Sigma-Aldrich. Table III also shows that T_m values of the blend remain close to the pure PLA except for that with 25%AP, the T_m is lowered by 4°C; however, higher compositions of AP brought T_{m} values closer to the 100% PLA. This is due to the fact that T_m value of pure AP is much

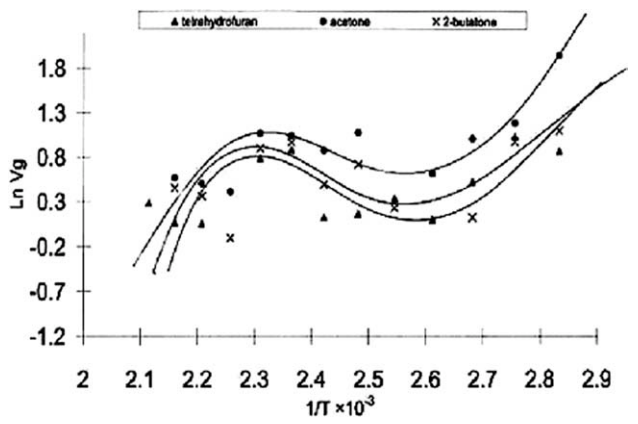

Figure 4 Retention diagram of pure AP–oxy solutes system (80–200°C).

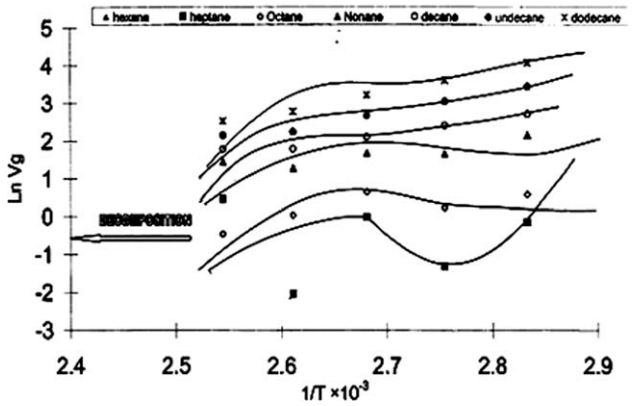

Figure 5 Retention diagram, blend of 75–25% AP–PLA–alkanes system at (80–120°C).

higher than that of pure PLA and because the degree of crystallinity of AP is much higher than that of PLA.

The transitions in the retention diagrams are not well pronounced to warrant the estimation of T_g values due to the kinetic effect of the diffusion of gases into the crystalline layer. However, Figure 2 shows a T_g value of 97°C for PLA and Figures 4 and 5 show a T_g value of 87°C for 75–25% and 50–50% of AP–PLA blends. This T_g value is lower than that of the pure PLA and AP. Thus, blending AP with PLA caused a decrease in T_g value due to the reduction of the degree of crystallinity of the blend.

Polymer–solute interaction parameters, χ_{12}

The interaction parameter, χ_{12}, was calculated for AP, PLA, and the blend–solutes systems according to Eq. (11). This parameter measures the strength of the specific interactions between the gaseous mobile phase and the polymer in the stationary phase. If these interactions are strong, the polymer and the solute are compatible (soluble) with each other, thus, negative χ_{12} values (exothermic) are expected. If the interactions are weak, χ_{12} is expected to be positive (endothermic) and a separation of the components is expected. Tables IV and V list χ_{12} of solutes' interactions with PLA, AP, and three weight fractions of AP–PLA blends in the temperature range at which the stationary phase is at melt. Therefore, the thermodynamic theories are valid in this zone due to the establishment of the equilibrium between the test solute and the polymer. Since pure PLA melts around 105°C, PLA-solutes χ_{12} was measured in the range of 100–130°C. Similarly, χ_{12} for pure AP was measured above the melt (170–200°C). χ_{12} for the three compositions of the blend was measured at 120°C above the region where a mixture of phases exist. PLA–solutes χ_{12} values hovered around the zero mark indicating that the interaction between PLA and all solutes used is exothermic. However, these values are narrow among the families, because each family represents a specific type of interactions or a combination of specific interactions. There are two more factors that contribute to this observation, one of which is the high molar mass of the polymers used; in particular, amylopectin (6.6 million g/mol). This factor makes the sorption of the vapor into the surface much more difficult especially when it is blended with PLA due to the reduction of the interaction sites available on the surface. The second factor is the strong interactions between the two polymers, makes the interaction sites even less available for the solute vapor. Alkanes and acetates showed an interesting trend as a number of carbons in the solute backbone increased, χ_{12} values were decreased. By adding a CH_2 group to the solutes' backbone, the dispersive forces increased and that led to more interactions with the PLA backbone. This is particularly true in the case of acetates by combining both the dispersive and the dipole-dipole forces which led to an even lower χ_{12} values than those of alkanes (Figure 8).

Due to the high molar mass and the complexity of AP's structure, the strength of the specific interactions of solutes with AP is not impressive as with

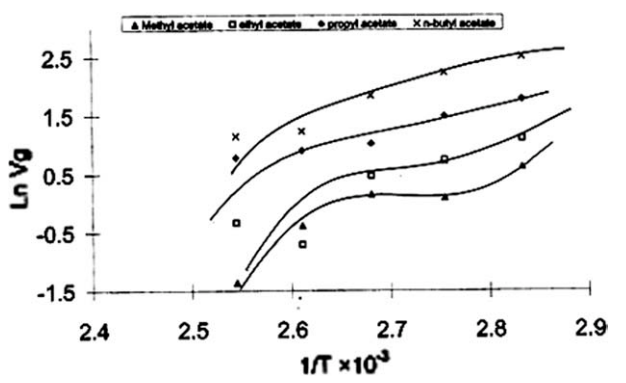

Figure 6 Retention diagram, blend of 50–50% AP–PLA–acetate systems at (80–120°C).

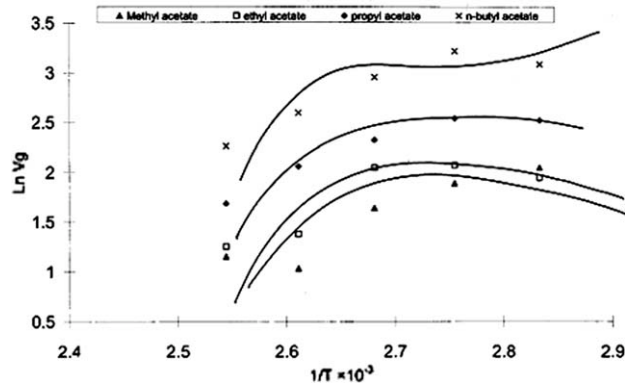

Figure 7 Retention diagram, blend of 25–75% AP–PLA–acetates systems at (80–120°C).

TABLE III
Melting Temperatures of Pure AP, Pure PLA, and Three of Compositions of AP-PLA Blends as Determined by IGC

Solutes	AP	AP75%–PLA25%	AP50%–PLA50%	AP25%–PLA75%	100%PLA
Alkanes	171	104	100	100.1	104
Acetates	174	104	102	100.1	104
Halogenated	162	100	102	100.1	107
Oxy group	162	105	102	100.1	104
Six-membered rings				100.1	105
Average	167.25	103.25	101.5	100.1	104.8

that of PLA. Table V shows that alkanes and acetates yielded endothermic interactions even at higher temperatures, whereas the oxy, halogenated and cyclic groups favor strong interactions, in particular, the oxy group for which χ_{12} values were close to zero at 130°C. However, due to the difficulty of finding Antoine constants in the literature at higher temperatures, χ_{12} values for this group cannot be computed.

χ_{12} values for three weight fractions of AP–PLA blends were also measured (Table V). In this case, χ_{12} is a measure of the strength of the specific interactions with two polymers combined and the whole system is considered to be a ternary system. All three blends showed χ_{12} close to zero due to the strong specific interactions with all solutes used. These values were decreased with increasing the number of carbon in the solutes' backbone in alkanes, which showed more favorable interactions than others unlike what was observed for the pure AP and PLA. Therefore, χ_{12} of the blend does not follow the same trend as of that for the pure polymers due to the complexity of the interaction sites on the surface of the blend as compared with those on the surface of the pure polymer. In other word, the blends surface is less polar than the pure polymer surfaces. Examination of Table VI reveal that a blend of 25%AP–75%PLA favors stronger interactions with the solutes than the other compositions; however, the differences in χ_{12} is small among the three compositions.

Polymer–polymer interaction parameters, χ_{23}

The compatibility (solubility) of a polymer pair is determined using the polymer–polymer interaction parameters, χ_{23}, and the contact energy parameter, B_{23} according to Eq. (15). χ_{23} parameter was calculated for the three weight fractions AP-PLA blends at 120°C above the melt. Table 6 shows strong

TABLE IV
Interaction Parameters

χ_{12} of PLA: Solute (100−130°C)					χ_{12} of AP: Solutes (170−200°C)				
Solutes	100	110	120	130	Solutes	170	180	190	200
NC_6	0.026	0.019	0.029		NC_6	1.01	2.99	0.34	0.88
NC_7	0.020	0.020	0.022		NC_7	1.32	1.85	1.61	0.72
NC_8	0.019	0.018	0.019	0.022	NC_8	1.82	2.04		1.32
NC_9	0.018	0.016	0.018	0.018	NC_9	1.72	1.75	1.18	0.99
C_{10}	0.017	0.016	0.016	0.015	C_{10}	2	2.28	1.48	1.05
C_{11}	0.016	0.015	0.015	0.015	C_{11}	2.35	2.78	1.83	N/A
C_{12}	0.015	0.015	0.015	0.014	C_{12}	2.6	2.44	2.18	2.07
MAC	0.028	0.023	0.025		MAC	0.25	0.28	0.43	0.35
EAC	0.020	0.019	0.022		EAC	1.2	1.32	0.31	0.75
PAC	0.017	0.016	0.020	0.017	PAC	1.2		0.95	0.88
NBA	0.015	0.015	0.016	0.015	NBA	1.35	2.26	1.48	0.17
THF	0.023	0.022	0.026		THF				
DOX	0.022	0.021	0.022	0.022	DOX				
ACT	0.026	0.027	0.037		ACT				
MEK	0.022	0.021	0.025		MEK				
C12	0.028	0.028			CL2	0.011		0.004	0.019
D12	0.023	0.024	0.024		D12				
CL3	0.024	0.022	0.024		CL3	0.034		0.016	0.015
CLB	0.019	0.020	0.020	0.020	PCL				
PCL	0.020	0.018	0.022	0.020	TCE	0.058		0.015	0.015
TCE	0.025	0.022	0.026		CHX				
CHX	0.025	0.022	0.024	0.028	CC6	0.027		0.015	0.028
CC6	0.026	0.023	0.027	0.026					
TOL	0.019	0.020	0.021	0.019					

TABLE V
Blends-Solute Interaction Parameters, χ_{12} (120°C)

Solutes	75%AP–25% PLA	50%AP–50% PLA	25%AP–75% PLA
Alkanes			
NC_6	0.022		0.017
NC_7	0.017		0.025
NC_8	0.024	0.022	0.017
NC_9	0.016	0.018	0.016
C_{10}	0.016	0.017	0.015
C_{11}	0.017	0.017	0.015
C_{12}	0.016	0.016	0.014
Acetates			
MAC	0.026		0.017
EAC	0.025	0.030	0.016
PAC	0.024	0.022	0.015
NBA	0.020	0.021	0.014
Oxy Group			
THF	0.029		0.016
DOX	0.024	0.030	0.018
ACT	0.030	0.022	0.022
MEK	0.030	0.021	0.022
Halogenated			
C12	0.029	0.030	0.020
D12	0.038	0.034	0.023
CL3	0.028	0.026	0.023
CLB	0.025	0.024	0.018
PCL	0.029	0.030	0.020
TCE	0.032	0.031	0.021
Six-member ring			
CHX	0.024		0.027
CC6	0.022	0.038	0.022
TOL	0.025	0.025	0.019

TABLE VI
Polymer–Polymer Interaction Parameters, χ_{23}, for Three Compositions AP−PLA Blends (120°C)

Solutes	75%AP–25%PLA	50%AP–50%PLA	25%AP–75%PLA
Alkanes			
NC_7	−2.95	−13.00	−7.13
NC_8	−11.74	−6.44	−2.55
NC_9	−3.88	−6.44	−2.05
C_{10}	−5.10	−3.67	−2.20
C_{11}	−5.10	−4.59	−2.85
C_{12}	−6.88	−4.56	−2.79
Acetates			
MAC			
EAC	−1.07	−4.59	−1.73
PAC	−7.69	−4.67	−0.21
NBA	−1.46	−3.57	−0.29
Oxy-group			
THF	−9.73	−1.90	
DOX	−0.76	−3.95	
ACT	−6.73	−10.94	
MEK	−3.74	−4.74	−0.88
Halogenated			
CL2	−1.57	−2.11	
TCE	−9.18	−2.78	−5.13
CL3	−1.11	−1.88	−1.27
PCL	−5.95		−0.88
D12	−0.10		
CLB	−1.79	−21.03	−0.38
BCL			
Six-member ring			
CC6		−4.54	
TOL	−4.89	−3.75	−1.17
CHX	−0.39	−0.40	−4.06

exothermic values of χ_{23} indicating the compatibility of AP and PLA at all weight fractions. Some boxes are left blank when Antoine constants are not available in the literature. The compatibility (miscibility) of the polymer pair using all solutes found to be coherent and the interactions between the polymer pair are strong according to our data. However, the degree of compatibility differed from one family to another and among the solutes within the family itself. However, the degree of compatibility differed from one family to another and among the solutes within the family itself. Values of χ_{23} are surprisingly negative an indication of the strong solubility of the two polymers due to the polarity of the two polymers, both provide ample interaction sites in the form of H-bonding. Generally speaking, there is no evidence of separation of the polymer pair at the measured temperature and weight fractions, and there are no absolute values of χ_{23} which can be drawn. This is due to the effect of the chemical nature of the solute on these two parameters as we first pointed out in earlier publications,[25] and

TABLE VII
Degree of Crystallinity of AP, PLA, and Blends (80–120°C)

Temperature (°C)	100 PLA	100P[a]	75%AP–25%PLA	50%AP–25%PLA	25%AP–75%PLA
84	88.12	98.00			81.18
87	83.80	97.00	99.46	98.07	73.82
91	82.09	96.00	98.96	97.29	66.71
94	75.34	90.00	96.49	96.08	59.34
97	65.35	88.00		91.95	46.21
101	54.16	86.00		84.28	30.23
104	47.80	87.00			13.93
108		86.00			
112		85.00			

[a] Data taken from ref. 1.

TABLE VIII
The Dispersive Surface Energy, γ_s^d, of Pure PLA and AP–PLA Blends (80–120°C)

	100% PLA			25%AP–75%PLA			50%AP–50%PLA			75%AP–25%PLA		
Temp (°C)	γ_{CH2}	ΔG_a^{CH2}	γ_s^d (mJ/m^2)	γ_{CH2}	ΔG_a^{CH2}	γ_s^d (mJ/m^2)	γ_{CH2}	ΔG_a^{CH2}	γ_s^d (mJ/m^2)	γ_{CH2}	ΔG_a^{CH2}	γ_s^d (mJ/m^2)
80	32.16	2304.8	31.62	32.16	2398.9	34.26	31.62	2351.5	32.91	32.16	2534.3	38.23
90	31.58	2087.4	26.41	31.58	2002.1	24.30	26.41	2328	32.85	31.58	2910.7	51.35
100	31.00	1923.8	22.85	31	1814.1	20.32	22.85	2594.3	41.56	31	2007.2	24.88
110	30.42	1954.7	24.04	30.42	2011.1	25.45	24.04	3045.5	58.36	30.42	2843.9	50.89
120	29.84	2158.3	29.88	29.84	2387.6	38.57	29.88	2021.3	26.21	29.84	1726.3	19.12

concluded that this effect is not of the IGC fault, but because of the limitation of the Flory–Huggins Theory due to the fact that this theory assumes that the Gibbs mixing function for the ternary polymer–polymer–solute system is additive with respect to the binary contributions.

Several IGC researchers discussed this effect and struggled to find a solution by which the effect of the chemical nature of solutes on these two parameters can be eliminated. Among these groups are as follows: Prolongo et al.,[35] Shi and Schreiber,[36] and Munk et al.[37] Much of the discussion was centered on the role of several types of interactions, such as dispersive forces, dipole–dipole and H-bonding, in determining these two parameters. Some introduced a corrective measure to treat the dependency of χ_{23} on the chemical nature of solutes taking into account the role of the surface and bulk compositions in multi-component polymer systems (blend). Also, considering that the partitioning of vapor-phase molecules between the components of the surface layer of a solid is likely to be nonrandom. Because the surface concentration of one polymer in the blend always exceeded the bulk composition (wt % ratio), the differences in these two parameters varied strongly with the choice of the vapor solute used. Another factor that contributes to these differences is the preferential adsorption of the host polymer (AP) on the chromatographic support and the migration of the diluent polymer (PLA) to the surface of the stationary phase.

To determine which family and weight fraction of the blend yielded the most exothermic values, χ_{23} of a variety of solutes' families were plotted versus the weight (mass) fraction of the blend in Figure 9. It is clear that the higher alkanes, propyl acetate, trichloroethylene and toluene, showed the most negative values at 25% mass fraction of PLA. At this composition, AP is in the dominant composition and PLA is only a diluent, yet, the interaction between the polymer pair is at highest due to the high molar mass of amylopectin. This observation was complemented with the high dispersive surface energy of this composition (next section).

Crystallinity

The degree of crystallinity of AP, PLA, and the three weight fractions of the blends in the temperature range of 80–120°C was measured from the retention diagrams such as Figures 1–7, by extrapolating the linear portion of the amorphous region (above T_m) to the crystalline region. Accordingly, two retention

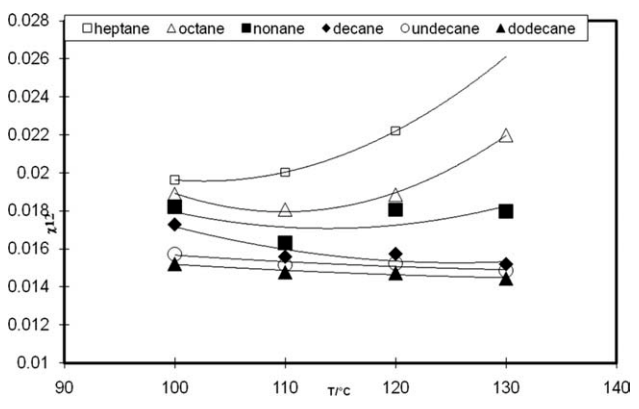

Figure 8 Dependence of the interaction parameter (χ_{12}) on temperature, for pure PLA–alkane system.

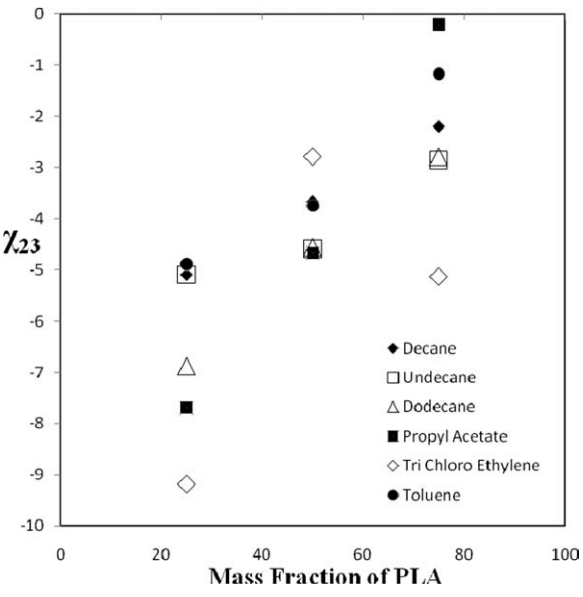

Figure 9 Dependence of χ_{23} on the mass fraction of the AP–PLA blend using a variety of solutes.

volumes can be measured: $V_{g,sample}$ is the retention volume of the solute in the crystalline region, and $V_{g,amorphous}$ is the retention volume of the solute in the extrapolated line of the amorphous region. By using the following relationship, the degree of the crystallinity can be assessed.

$$\%X_c = 100\left\{1 - \left\{\frac{V_{g,sample}}{V_{g,amorphous}}\right\}\right\} \quad (19)$$

Using Eq. (19), the degree of crystallinity of the three blends was compared with that of the pure AP and PLA. Table XII shows that both AP and PLA are crystalline at 84°C; however, AP remains crystalline as the temperature increased to 120°C, unlike PLA, the degree of crystallinity decreased significantly at 120°C. Blending 75%AP–25%PLA and 50%AP–50%PLA did not influence the degree of crystallinity; both compositions remain crystalline at 100°C. The third composition of 25%AP–75% PLA followed the others compositions' trend; the degree of crystallinity is significantly reduced with increasing temperature and the small amount of AP did not affect this reduction. Hence, a correlation between the degree of crystallinity and the compatibility of the blend can be drawn. These findings agree well with Table III data of melting point. This composition showed the lowest melting temperatures among the three compositions of the blend.

Surface energy

The dispersive component of the surface energy of AP, PLA, and the three compositions of the blends were calculated using only the alkane series in the temperature range of 80–120°C. According to Eq. (17), plots of ($RT \ln V_g^o$) in KJ/mol versus the number of carbons in the alkane series were generated for each temperature. Linear relationships were obtained in all of these plots, and the slope of the straight lines were computed as the free energy of adsorption of a CH_2 group, ΔG_a^{CH2}. Utilizing Eq. (20), the dispersive component of the surface energy of AP–PLA blends, γ_d^s, was calculated as a function of temperature. The cross-sectional area[20] of an adsorbed CH_2 group, a_{CH2} is estimated to be 6 $(Å)^2$. The surface-free energy of a solid containing only CH_2 groups, γ_{CH2}, is computed as a function of temperature as follows:

$$\gamma_{CH2} = 36.80 - 0.058t \quad (20)$$

where t is the temperature in °C. Table XIII compares the dispersive surface energy of the 100% AP, 100% PLA, and three blends at 80–120°C. γ_d^s values ranged from 31 mJ/m^2 for pure PLA as compared with 16.09 mJ/m^2 the pure AP[1] at 80°C and ranged from 34 to 38 mJ/m^2 among the three compositions. All γ_d^s values decreased with temperature due to the thermal expansion of the polymer surface above the melt. Once again composition 75%AP–25%PLA showed the larger values of γ_d^s agreeing well with χ_{23} values.

CONCLUSIONS

The morphology changes, polymer solute interactions, polymer–polymer interactions, crystallinity and dispersive component of the surface energy of AP, PLA, and three weight fractions of AP–PLA were studied using the IGC method. In this article, IGC was found to be capable of determining those characteristics of a complex polymeric system, it complimented the DSC method in obtaining the T_g and T_m values of a high molar mass starch based polymer, AP, and its blend with PLA. The miscibility of AP and PLA is found to be favorable at 75%AP–25%PLA. That was evident from two observations complemented each others, they are as follows: χ_{23} values and the dispersive component of the surface energy.

The degree of crystallinity of AP was important in explaining the low values of the surface energy found by IGC and the improvement of γ_d^s values when AP was blended with PLA. The IGC was also able to measure the interaction parameters, χ_{12}, of 25 solutes representing a variety of families with different chemical natures over a wide temperature range and composition; this measurements determined the solubility of the pure AP, pure PLA, and AP–PLA blends in these solutes. It was also able to determine the blends' compatibility (solubility) over a wide range of temperature and weight fractions.

References

1. Al-Ghamdi, A.; Melibari, M.; Al-Saigh, Z. Y. J App Polymer Sci 2006, 101, 3076.
2. Holmes, P. A. Developments in Crystalline Polymers, Vol. 2; London, UK: D.C. Bassett Elsevier, 1988; pp 1–65.
3. Doi, Y. Microbial, Polyesters; New York: VCH Publishers; 1990.
4. Holmes, P. A. Phys Technol 1985, 16, 32.
5. Follain, N.; Joly, C.; Dole, P.; Bliard, C. J Appl Polym Sci 2005, 97, 1783.
6. Zhang, L.; Deng, X.; Zhao, S.; Huang, Z. Polym Inter 1997, 44, 104.
7. Fanta, G. F.; Swanson, C. L.; Doane, W. M. J Appl Polym Sci 1990, 40, 811.
8. Shogren, R. L.; Thompson, A. R. J Appl Polym Sci 1992, 4, 1971.
9. Shogren, R. L.; Greene, R. V.; Wu, Y. V. J Appl Polym Sci 1991, 42, 1701.
10. Alghamdi, A.; Melibari, M.; Al-Saigh, Z. Y. J Polym Environ 2005, 13, 319.
11. Han, X.; Ma, X.; Liu, J.; Li, H. Carbohydr Polym 2009, 78, 533.
12. Al-Saigh, Z. Y. Inter J Polym Character Anal 1997, 3, 249.
13. Al-Saigh, Z. Y.; Guillet, J. In Encyclopedia of Analytical Chemistry: Instrumentation and Applications; Meyers, R., Ed., Vol. 9; Chichester: Wiley; 2000, pp 7759–7792.
14. Al-Saigh, Z. Y. Polym Inter 1996, 40, 25.
15. Al-Saigh, Z. Y. Polymer 1999, 40, 3479.
16. Chehimi, M.M.; Pigois-Landureau, E.; Delamar, M.M. J Chim Phys 1992, 89, 1173.
17. Landureau, E.; Chehimi, M. M. J Appl Polym Sci 1993, 49, 183.

18. Chehimi, M. M.; Abel, M. L.; Perruchot, C.; Delamar, M.; Lascelles, S. F.; Armes, S. P. Synth Met 1999, 104, 51.
19. Papirer, E.; Eckhardt, A.; Muller, F.; Yvon, J. J Mater Sci 1990, 25, 5109.
20. Papirer, E.; Ligner, G.; Vidal, A.; Balard, H.; Mauss, F. In Chemically Modified Oxide Surfaces; Leyden, E., Collins, W.T., Eds. New York: Gordon and Breach, 1990; 361.
21. Papirer, E.; Balard, H.; Vidal, A. Eur Polym Mater 1988, 24, 783.
22. Papirer, E.; Roland, P.; Nardin, M.; Balard, H. J Colloid Interface Sci 1986, 113, 62.
23. Al-Saigh, Z. Y.; Chen, P. Macromolecules 1991, 24, 3788.
24. Al-Gahmdi, A.; Al-Saigh, Z. Y. J Polym Sci Part B: Polym Phys 2000, B38, 1155.
25. Al-Saigh, Z. Y.; Munk, P. Macromolecules 1984, 17, 803.
26. Thielmann, F. J Chromatogr A 2004, 1037.
27. Papirer, E.; Brendle, E.; Ballard, H.; Vergelati, C. J Adhesion Sci Technol 2000, 14, 321.
28. Balard, H.; Brendle, E.; Vergelati, C. In Proceedings of 3rd International Wood and Natural Fiber Composites Symposium, September, Kassel, Germany, 2000.
29. Al-Saigh, Z. Y. In Degradable Polymers and Materials Principles and Practice; Khemami, K., Scholz, C., Eds; Washington: ACS Symposium Series No. 939, 2006; Chapter 20.
30. Munk, P. In Modern Method of Polymer Characterization, Vol. 113; Barth, H. G., Mays, J. W., Eds.; New York: Wiley, 1991; pp 151–200.
31. Flory, P. J. Principles of Polymer Chemistry; Ithaca, NY: Cornell University Press, 1953.
32. Fowkes, F. W. Ind Eng Chem 1964, 561, 40.
33. Fowkes, F. W. Ind Eng Chem Prod Res Dev 1967, 56, 40.
34. Card, T. W.; Al-Saigh, Z. Y.; Munk, P. J Chromatograph 1984, 301, 261.
35. Prolongo, M. G.; Masegosa, R. M.; Horta, A. Macromolecules, 1989, 22, 4346.
36. Shi, Z. H.; Schreiber, H. P. Macromolecules 1991, 24, 3522.
37. Munk, P.; Hattam, P.; Abdual-Azim, A.; Du, Q. Makromol Chem Macromol Symp 1990, 38, 205.